

Microstructure characterization of oxide dispersion strengthened Alloy 617

Y.B. Chun*, C.H. Han, B.Y. Lee, J. Jang

Nuclear Development Division, Korea Atomic Energy Research Institute
 1045 Deadeok-daero, Yuseong-gu, Daejeon 305-353, South Korea

*Corresponding author: youngbumchun@kaeri.re.kr

1. Introduction

Nickel based alloys are considered the reference candidate materials for high temperature gas-cooled reactors which should work under very high harsh conditions, i.e., temperatures above 900 °C and internal gas pressures higher than ~8 MPa [1]. According to a recent investigation, no proven industrial technology could be directly used for such applications. For example, extensive work on Alloy 617 which is the candidate material for the intermediate heat exchanger (IHX) in very high temperature reactors (VHTR) shows that Alloy 617 exhibit quite good creep properties [2-4], the maximum service temperature of Alloy 617 is much less than that required for the VHTR-IHX applications. In this regard, oxide dispersion strengthened (ODS) materials have received a great attention owing to their excellent mechanical properties at higher temperatures, e.g., creep resistance. As part of an alloy development program for nickel base ODS alloy, we have produced an ODS Alloy 617 via mechanical alloying and hot extrusion, and characterized its microstructural evolution during the process and evaluated mechanical properties at elevated temperatures. The current work reports the effects of the solution treatment temperature on the microstructural evolution of the ODS Alloy 617.

2. Methods and Results

2.1 Experimental procedures

An ODS Alloy 617 with the chemical composition given in Table 1 was produced based on a powder metallurgy method and hot extrusion. Prealloyed powder with the chemical composition the same to Alloy 617 was produced by atomization. A mixture of the prealloyed powder and 0.6 wt.% yttria was mechanically alloyed (MA) by milling with steel balls (steel ball to powder ratio is 15:1 in weight) at 200 rpm for 40 h. in a Simoloyer CM08 horizontal mill.

Table I: Chemical composition of experimental ODS Alloy 617 in weight percent.

Cr	Co	Mo	Fe	Al
22	12.5	9	1.5	1
Ti	C	B	Y ₂ O ₃	Ni
0.4	0.1	0.003	0.6	Bal.

The MA powders thus prepared were sealed in a mild steel container and degassed at 400 °C for 1h under a vacuum of 10⁻⁴ torr. The steel container filled with MA powders was pre-heated at 1000 °C for 2h and then hot extruded with a reduction ratio of 6.25:1. The extruded bar was solution treated at temperature between 1100 °C and 1350 °C.

Microstructures of the MA powder and the extruded bar were characterized using scanning electron microscope (SEM), and the chemical compositions of precipitates formed were quantified using an energy-dispersive X-ray spectroscopy (EDS). Texture evolution during solution treatment was analyzed using an electron backscattering diffraction (EBSD) technique. An EBSD analysis was undertaken using a FEI 3D Quanta field-emission-gun (FEG) SEM equipped with a TSL-OIM™ data acquisition system. Samples for the electron microscopy were mechanically ground and then further polished with an alumina suspension. All the analyses were conducted on the section normal to the radial direction of the extruded round bar.

2.2 Results and Discussion

Mechanical alloying produced irregularly-shaped MA particles (Fig. 1(a)). A characteristic morphology (Fig. 1(b)) suggests a repeated fragmentation and welding [5]. The size of MA particles ranges from a few μm to ~100 μm, the average being ~25 μm (Fig. 1(c)).

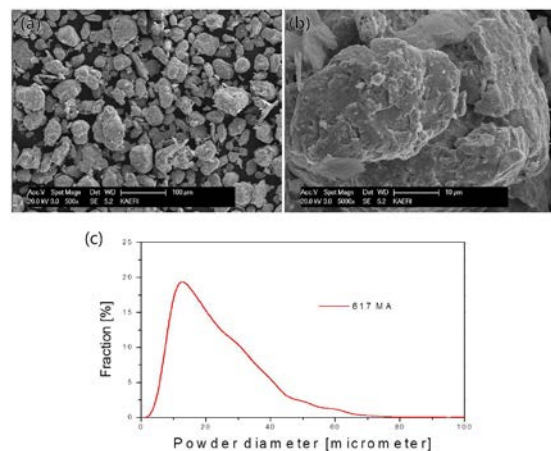


Fig. 1. SEM micrographs of MA powder at (a) low (X500) and (b) high (X 5,000) magnifications, and the size distribution of particles.

An EDS analysis revealed a quite homogeneous distribution of the major alloying elements with a MA particle (Fig. 2), although local segregation of an alloying elements was observed in some particles, e.g., segregation of iron in Fig. 2.

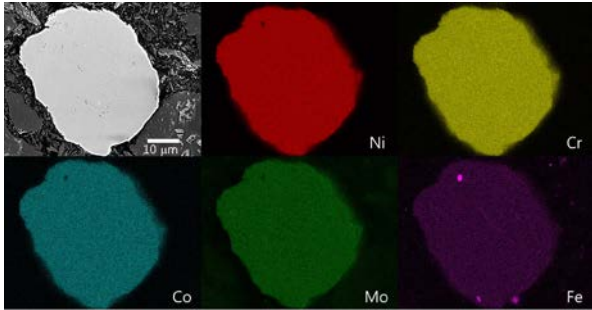


Fig. 2. Results of EDS mapping for a MA particle: the spatial distribution of the major alloying elements (Ni, Cr, Co, Mo and Fe) within a MA particle.

In as hot-extruded condition, the ODS Alloy 617 contained globular $\text{Cr}(\text{Ni},\text{Co})_{23}\text{C}_6$ carbides and fine Al-based oxides, which appear dark and bright contrast, respectively, in Fig. 3(a). With increasing temperatures up to 1200 °C, the both $\text{Cr}(\text{Ni},\text{Co})_{23}\text{C}_6$ carbides and Al-based oxides coarsened and the number density of which decreased (Figs 3(b) and 3(c)).

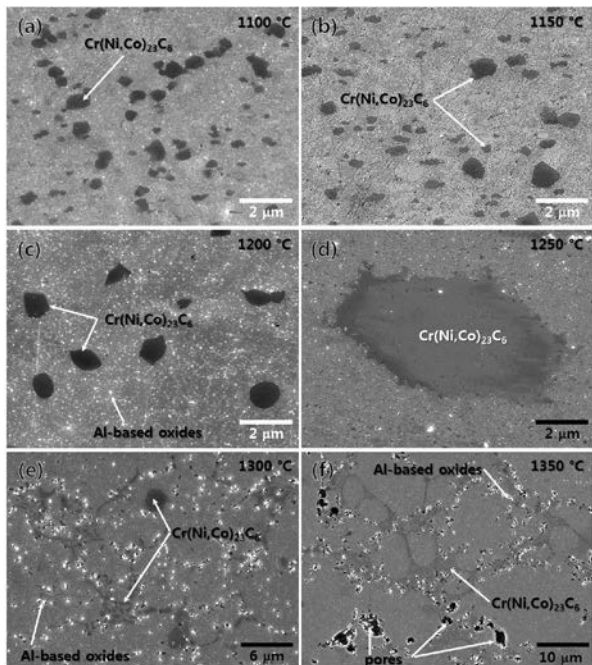


Fig. 3. Evolution of carbides and Al-based oxides with the solution treatment temperatures: (a) 1100 °C, (b) 1150 °C, (c) 1200 °C, (d) 1250 °C, (e) 1300 °C, and (f) 1350 °C. All the samples were solution treated for 1h and then water-quenched.

When solution treated at 1250 °C, the $\text{Cr}(\text{Ni},\text{Co})_{23}\text{C}_6$ carbides grew into hexagonal-prism shape and, as a result, both rod-like and hexagon-shaped (Fig. 3(d)) carbides were observed in the two-dimensional micrograph. Further increase in the solution treatment temperatures up to 1350 °C, the hexagonal-prism shaped carbides changed their form into eutectic structure (Fig. 3(e) and 3(f)), which is, however, accompanied with formation of pores.

The hot-extruded sample showed a very fine grain structure (Fig. 4(a)). The EBSD results showed that the grain size ranges from 0.1 μm to 5 μm, the average being ~0.4 μm. Hot extrusion of the MA powder developed {111} fiber texture where the <111> direction of grains is aligned preferentially to the extrusion direction (Fig. 4(b)). However, the texture intensity is very weak, the maximum pole intensity being ~ 1.5. This can be attributed to the small extrusion ratio imposed.

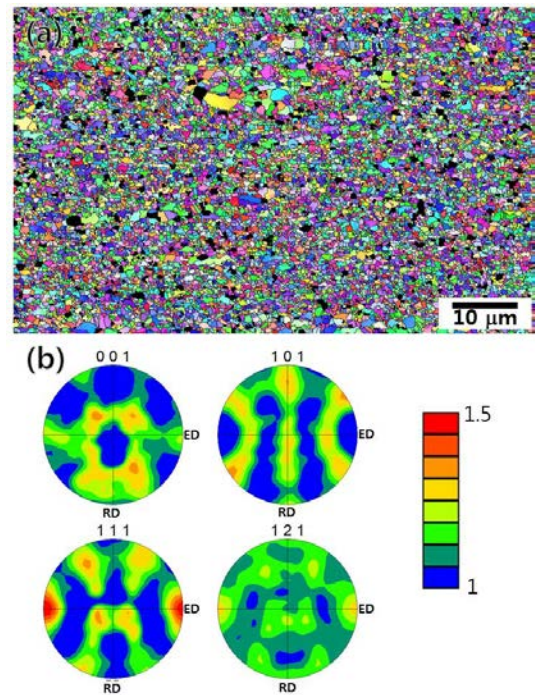


Fig. 4. EBSD results of the as hot-extruded ODS Alloy 617: (a) inverse pole figure map for the radial direction and (b) {001}, {110}, {111} and {112} pole figures. Black areas in (a) corresponds to locations where carbides reside.

When solution treated at 1200 °C for 1h, some grain showed an abnormal grain growth, whereas only slight growth was observed for the other grains (Fig. 5(a)). The abnormal grain growth took place in a local region, resulting in an elongated agglomerate of coarse grains. This can be ascribed to local depletion of oxides particles that play a pinning role of grain boundaries. The coarse grains (avg. grain size ~ 10 μm) contained

lots of annealing twins inside, which suggests rapid migration of grain boundaries during the solution treatment. The average grain size of grains other than the abnormally-grown grains is $\sim 0.8 \mu\text{m}$. Such small grains also contained annealing twins inside.

The solution treatment weakened the texture of hot-extruded sample. The pole figures given in Fig. 5(b) suggest a slight randomization of texture, which is attributed to the formation of annealing twins. Increase of the maximum pole intensity to 3 is simply due to the coarse grains in the microstructure.

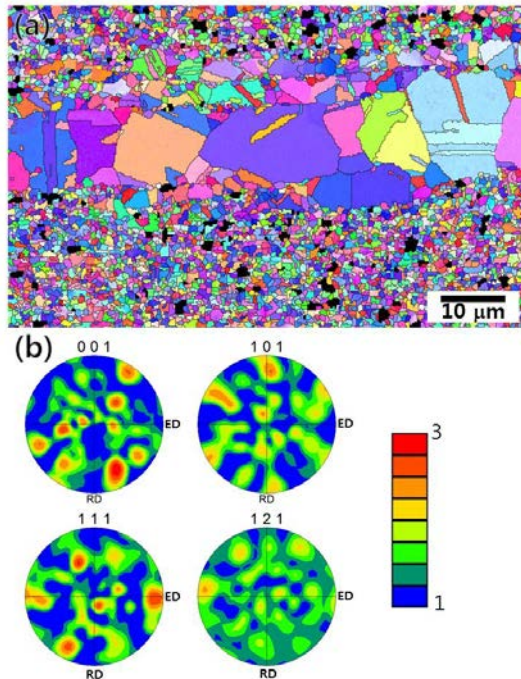


Fig. 5. EBSD results of the as solution-treated (1200 °C/1h) ODS Alloy 617: (a) inverse pole figure map for the radial direction and (b) {001}, {110}, {111} and {112} pole figures. Black areas in (a) corresponds to locations where carbides reside.

3. Summary

The microstructure evolution of ODS Alloy 617 during solution treatment was characterized. In hot-extruded condition, the alloy consisted of submicron-sized fine grains, globular $\text{Cr}(\text{Ni},\text{Co})_{23}\text{C}_6$ carbides and Al-based oxides. The subsequent solution treatment led to a slight growth of grains but in local regions there were abnormal grain growth. Solution treatment coarsened carbides during which the morphology of carbides was changed from globular shape to eutectic structure via hexagonal prism.

REFERENCES

[1] P. Yvon, F. Carré, Structural materials challenges for advanced reactor systems, *Journal of Nuclear Materials*, Vol. 385, p. 217, 2009.

[2] W-G. Kim, J-Y. Park, I.M. W. Ekaputra, M-H. Kim, Y-W. Kim, Analysis of Creep Behavior of Alloy 617 for Use of VHTR Systems, *Procedia Materials Science*, Vol. 3, p. 1285, 2014.

[3] G-G. Lee, S. Jung, J-Y. Park, W-G. Kim, S-D. Hong, Y-W. Kim, Microstructural Investigation of Alloy 617 Creep-ruptured at High Temperature in a Helium Environment, *Journal of Materials Science and Technology*, Vol. 29, p. 1177, 2013.

[4] L.J. Carroll, C. Cabet, M.C. Carroll, R.N. Wright, The development of microstructural damage during high temperature creep-fatigue of a nickel alloy, *International Journal of Fatigue*, Vol. 47, p. 115, 2013.

[5] C. Suryanarayana, Mechanical alloying and milling, *Progress in Materials Science*, Vol. 46, p. 1, 2001.